Prediction of thermal protection system material permeability and hydraulic tortuosity factor using Direct Simulation Monte Carlo

Revathi Jambunathan[*], Deborah A. Levin[†], Arnaud Borner[‡], Joseph C. Ferguson[§], and Francesco Panerai[¶]

Carbon preforms used in Thermal Protection System (TPS) materials are 80 to 90% porous, allowing for boundary layer and pyrolysis gases to flow through the porous regions. The bulk material properties such as permeability and hydraulic tortuosity factor affect the transport of the boundary layer gases. The use of Direct Simulation Monte Carlo along with the Klinkenberg permeability formulation allows us to compute the continuum permeability and Knudsen correction factor for flow in the transition regime. In this work, we have computed the permeability for two types of carbon preforms, namely, Morgan Felt and FiberForm, and assessed the effect of orientation on the permeability. Since both the materials are anisotropic, the permeability was found to depend on orientation, wherein, the materials are more permeable in the in-plane orientation than the through-thickness orientation. The through-thickness orientation was also more tortuous compared to the in-plane material orientation. Compared to Morgan Felt, FiberForm is less permeable, in both, through thickness and in-plane directions.

[*]Graduate Student, Department of Aerospace Engineering, University of Illinois, Urbana-Champaign, IL-61801, AIAA Student Member.,

[†]Professor, Department of Aerospace Engineering, University of Illinois, Urbana-Champaign, IL-61801, AIAA Fellow

[‡]Reseach Scientist, STC at NASA Ames Research Center, MS258-6, Moffett Field, CA, 94035, USA, AIAA Member

[§]Junior Research Scientist, STC at NASA Ames Research Center, MS258-6, Moffett Field, CA, 94035, USA

[¶]Research Scientist, AMA Inc. at NASA Ames Research Center, MS234-1, Moffett Field, CA, 94035, USA, AIAA Member.

I. Introduction

Spacecraft are exposed to aerothermodynamic heating during entry into a planetary atmosphere and require thermal protection systems (TPS) to shield the vehicle and its crew from the chemically reacting high temperature gases. Candidate TPS materials, such as the Phenolic Impregnated Carbon Ablator (PICA)[1,2] are composed of a complex network of carbon fibers of micrometer size impregnated with a phenolic resin. These TPS materials undergo ablation, a self-sacrificial process, to protect the vehicle. Characterizing the material morphology and predicting its permeability and tortuosity factor is critical in modeling the transport of high temperature gases through the material, as well as the material response. The main objective of this work is to compute the material permeability and hydraulic pressure driven tortuosity factor of porous preforms used in TPS materials, namely Morgan carbon felt[3] (Morgan Advanced Materials, Fostoria, Ohio,USA) and FiberForm®[3] (Fiber Materials, Inc.). In addition we aim at determining the representative elementary volume (REV) for each microstructure so that, material analysis can be performed on smaller samples without compromising on the accuracy of the computed material properties. We will analyze the effect of material orientation on the material properties, since these fibrous microstructures are known to be anisotropic.[4,5] The small characteristic length scale of this problem renders the flow to be at non-continuum regimes even at atmospheric pressures requiring the use of more accurate kinetic theory based approaches to solve the transport within porous microstructure.

Direct Simulation Monte Carlo[6] (DSMC) is a probabilistic particle-based method that provides a numerical solution to the Boltzmann transport equation which accurately models finite Knudsen number flows. The gas flow is simulated by computational particles, where each particle represents a large number of real atoms or molecules. Traditionally, the computational domain is divided using a uniform Cartesian grid such that the cell size is less than

the local mean free path, in order to satisfy the DSMC criteria. At every timestep, particles are moved, sorted into nearest neighbors or cells, and binary collisions are performed between particles that belong to the same cell. For problems with sharp density gradients, a uniform grid would have to refine the cells everywhere in the domain, thereby over-refining the cells in some regions and increasing the computational time. To reduce the computational time, more recently, adaptive mesh refinement has been implemented, where cells are refined only in the regions where the local mean free path is small. However, for accurately modeling flow through highly irregular bodies, an octree-based solver is an advantageous approach when combined with additional capabilities such as volume-of-fluid and ray-tracing to determine the exact fluid volume of cut-cells and for gas-surface interactions. Even with efficient octree approaches, performing DSMC calculations for flow through fibrous microstructures is computationally expensive and novel parallelization strategies are required to reduce simulation run-time. In an effort to improve the computational efficiency, we have developed a scalable three-dimensional DSMC solver called Cuda-based Hybrid Approach for Octree Simulations (CHAOS),[7] to accurately model the flow through irregular porous media and exploit the heterogeneous architectures available in many petascale supercomputers.[8] In the CHAOS DSMC solver, linearized octrees are employed to efficiently account for multiple length scales. Large number of gas-surface interactions between the gas and TPS material are modeled using ray-tracing algorithms, using massively parallel methods on multiple GPUs. In our previous work,[7] we have shown 85% strong scaling and nearly 100% weak scaling with CHAOS for flow through the fibrous microstructures.

II. Numerical Method and Test Cases

The target problem involves computing morphological properties of two materials, namely, FiberForm and Morgan felt.[3,5,9] Figure 1 shows a computational model of the felt and

FiberForm TPS materials. They were obtained using a tomography image that was surface rendered and converted into a standard stl format with an average of 4 million triangular surface elements. These models allow us to compute permeability,[9–11] which is an important material property that controls the transport process of boundary layer and pyrolysis gases, which in turn enables the prediction of heat transfer to the material and the resulting degradation. Similarly, the hydraulic tortuosity factor[12–14] is a critical geometrical parameter as it quantifies how the gas particles deviate from a straight path to flow through the irregular pores of the material in a pressure driven flow. This hydraulic pressure driven tortuosity factor can be used to determine the hydraulic diameter[15] of porous materials, which in turn is used to obtain the Reynolds number and friction factor[15] in pressure driven flow through porous media. From micro-tomography measurements, Panerai *et al.*,[9] showed that the porosity for FiberForm is nearly 85-91% and that of the felt is 94%. Borner *et al.*,[5] used DSMC simulations to compute the permeability of the fibrous microstructures, predicting a higher permeability for the Morgan felt as compared to FirberForm. It was also shown, both from experiments[9] and previous DSMC[5] computations that both, the Morgan Felt and FiberForm material have a transverse isotropic structure, that is, the through-thickness (TT) orientation is less permeable than the in-plane (IP) direction. That is due to the manufracturing process of these materials, in which the billet is compressed in one direction. The DSMC simulations were performed on a smaller sample size of (520×520×520) μm^3. However, in the current work, due to the capability of CHAOS DSMC solver to handle large sample sizes, we will compute the material permeability and hydraulic tortuosity factor on a (1×1×1) mm^3 material sample and also determine the REV, that is, the smallest sample size that can be used for analysis without significantly affecting the predicted macroscopic transport properties of the material.

The definition of the DSMC test cases performed on the two materials, Morgan felt and FiberForm, to study the effect of temperature, sample size and orientation, are given in

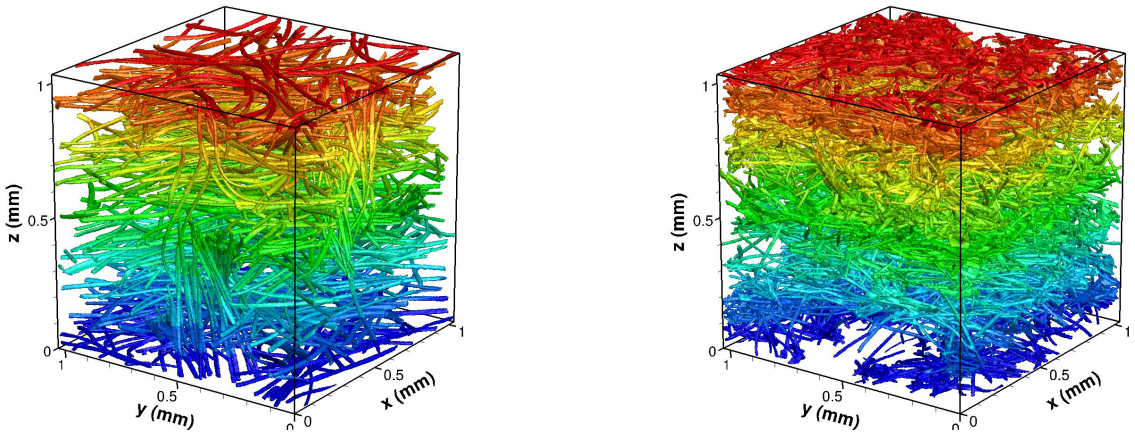

(a) Morgan felt microstructure reconstructed using 2.6 million surface mesh elements.

(b) FiberForm® microstructure reconstructed using 5.6 million surface mesh elements.

Figure 1: Fibrous microstructure reconstructed from tomography images of candidate TPS materials. Red to blue color scale represents increasing distance from the top surface. The TT direction is along the z-axis, and the IP direction is along the x or y-axis.

Tabs. 1 and 2. Test cases Felt 1 and 2 were performed on the large 1 mm^3 material to study the effect of orientation on continuum permeability. To study the effect of sample size, the $K_{o,TT}$ obtained for the large sample size in test case Felt 1 is compared with the DSMC calculations performed by Borner *et al.*,[5] for a smaller sample size of (520×520×520) µm^3. The DSMC computations performed by Borner *et al.*,[5] used an initial gas and surface of 300 K, while, in contrast, the CHAOS DSMC simulations performed in this work use different initial gas and surface temperature at 2000 and 300 K, respectively. However, since in the simulations performed in this work, the material surface was maintained at 300 K throughout the DSMC computation and the gas-surface interactions were fully diffuse, the gas temperature within the porous material is expected to equilibrate with that of the surface temperature. For the FiberForm material, four test cases are performed using CHAOS DSMC as shown in Table 2. Test cases Form 1 and 2 are performed for the large 1 mm^3 sample with different initial gas and surface temperature to study the effect of orientation on the continuum permeability. To study the effect of initial gas and surface temperature on the TT continuum permeability, test case Form 3 is performed with initial gas and surface

temperature at 1319 K, similar to the permeability experiments performed by Panerai *et al.*,[9] on a 22 mm^3 sample. Additionally, test case Form 4 is performed for a sample size of 520 μm^3 with initial gas and surface at 1319 K, to study the effect of sample size on the TT continuum permeability, compared to Form 3.

Table 1: Test case definition for Morgan felt

Test Case	Orientation	Sample Size (μm^3)	Initial T_g and T_s
Felt 1	TT	1032×1032×1032	T_g=2000 K, T_s=300 K
Felt 2	IP	1032×1032×1032	T_g=2000 K, T_s=300 K

Table 2: Test case definition for FiberForm

Test Case	Orientation	Sample Size (μm^3)	Initial T_g and T_s
Form 1	TT	1032×1032×1032	T_g=2000 K, T_s=300 K
Form 2	IP	1032×1032×1032	T_g=2000 K, T_s=300 K
Form 3	TT	1032×1032×1032	T_g=1319 K, T_s=1319 K
Form 4	TT	520×520×520	T_g=1319 K, T_s=1319 K

For all the above defined test cases, argon gas particles are introduced at the domain inlet with an initial bulk velocity of 460 m/s in the negative z-direction for the TT calculations and in the +x-direction for the IP computations, with an initial gas temperature, T_g. Since the geometry is irregular, non-periodic, and represents only a small sample of the bulk material, a pseudo-periodic boundary condition, also called mirror boundary condition, is imposed on the cross-stream boundaries. For this boundary condition, when particles cross the boundary after movement, they are specularly reflected back into the domain, instead of allowing them to enter from its opposite plane, which we call as the periodic counterpart. This pseudo-periodic assumption holds true in our simulations because, on average, the total number and total energy of particles that leave the domain from one cross-stream boundary is equal to the total number and total energy of outgoing particles from its periodic counterpart. For all the DSMC simulations, the material microstructure is assumed to be stationary with a

constant surface temperature, T_s. When gas particles collide with the material surface, they are reflected diffusely with energy equivalent to the surface energy.

III. Material Permeability and Hydraulic Tortuosity Results

To enable the comparison of fully kinetic simulation results with the experiments[9] of gas transport through porous media, the Klinkenberg formulation[10,11] is used to estimate the effective permeability, K, of the TPS material, which accounts for rarefied slip effects, and is given as[11],

$$K = K_o[1 + (b/P_{av})], \tag{1}$$

where, b is the permeability slip parameter or Knudsen correction factor that varies with temperature and gas composition, K_o is the continuum permeability, and P_{av} is the average gas pressure in the domain. K_o is strictly a function of the material microstructure, while b depends on both, the microstructure and the gas flow conditions. From Darcy's law, continuity equation, and the ideal gas law, the mass flow rate and permeability are related as follows,[11]

$$F = \frac{\mu \dot{m} RTL}{AM\Delta P} = K_o(P_{av} + b) \tag{2}$$

where, the permeability force F can be used to graphically relate K_o, P_{av}, and b by substituting the values of mass flow rate, $\dot{m}$, temperature, T, and the pressure difference between the inlet and outlet, ΔP, obtained from the DSMC calculations. Since the viscosity coefficient, μ, molar gas constant, R, the molar mass, M, of the gas species, the length L and cross-sectional area of the domain, A, are known, the values of K_o and b are obtained from a linear least-squares fit of F vs P_{av} values from DSMC calculations performed for different

average pressures. The continuum permeability, K_o, is computed by taking the slope of F vs P_{av} and the value y-intercept gives the permeability slip parameter. The values of K_o and b obtained for the test cases Felt 1 and 2, and for cases Form 1-4, are discussed in subsections III A and B.

A. Effect of orientation, size and temperature on Permeability of Morgan Felt

DSMC simulations are performed with different average pressures for the 1 mm^3 Morgan felt material, in both the through-thickness (TT) and in-plane (IP) directions. The variation of the permeability force, F, obtained by substituting values from the DSMC simulations in Eq. (2), for different average pressures are shown in Figs. 2(a) and 2(b) for test cases Felt 1 and Felt 2, respectively. The continuum permeability of the material is obtained from the slope of the line and the y-intercept gives the Knudsen correction factor, b. It is found that the continuum permeability, K_o, of Morgan felt, is 209.9×10^{-12} m^2 in the TT direction, with b =7027.15 Pa. In the IP direction, the continuum permeability is higher, $K_o = 271.8 \times 10^{-12}$ m^2 with b =5896.69 Pa, as compared in Tab. 3. The permeability is higher in the IP direction compared to the TT direction due to the anisotropic alignment of the fibers. Since the permeability is higher in the TT direction, the number of gas-surface interactions in TT are larger than in IP, thereby increasing the Knudsen correction factor, b, in the TT direction.

The TT continuum permeability obtained for the large 1 mm^3 felt material is compared to the TT continuum permeability obtained by Borner *et al.*,[5] for a smaller material volume of (520×520×520) μm^3 in Tab. 3. Note that, Borner *et al.*,[5] performed DSMC simulations with equal gas and surface temperature at 300 K, whereas for the Felt 2 case the initial gas temperature used was 2,000 K with surface temperature equal to 300 K. It can be observed that the continuum permeability of Morgan felt obtained for the larger material from CHAOS DSMC is approximately 7% higher than that obtained from the DSMC computation

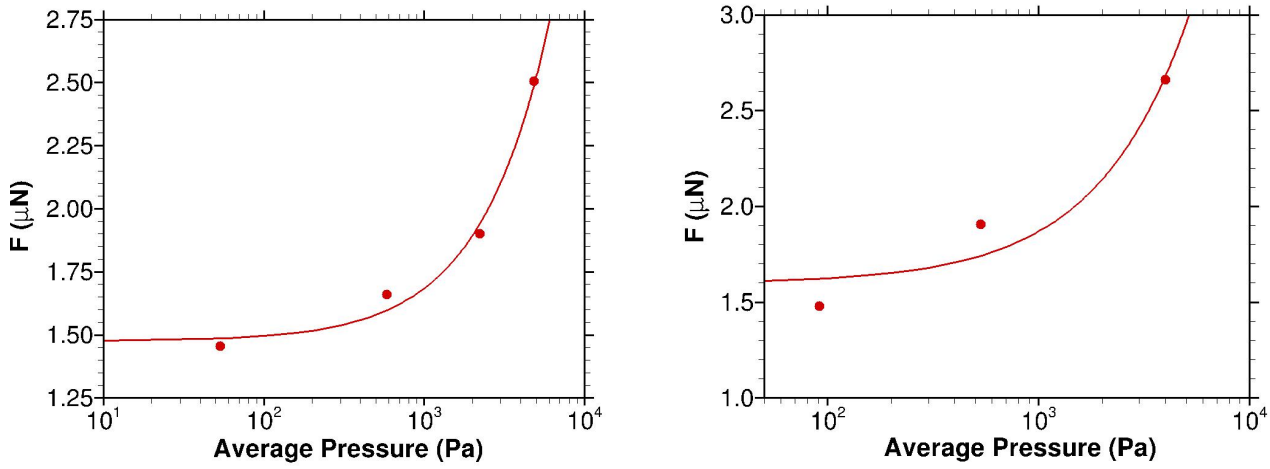

(a) F versus average pressure in the TT direction. $K_{o,TT}$=209.9×10^{-12} m^2, b=7027.15 Pa.

(b) F versus average pressure in the IP direction. $K_{o,IP}$=271×10^{-12} m^2, b=5896.67 Pa.

Figure 2: Continuum permeability K_o and Knudsen correction factor, b, of Morgan Felt in TT and IP.

performed by Borner *et al.*,[5] for a smaller material sample. Since the difference in material permeability is within the uncertainty of ±10%, a smaller material sample of 520 µm^3 may be sufficient to compute the material permeability for Morgan felt. The Knudsen correction factor, however, is higher in CHAOS compared to the results obtained from Borner *et al.*[5] Unlike the continuum permeability, which is a material property, the b factor is affected by the gas temperature, which is approximately 300 K within the material pores, but higher at the inlet of the computational domain and at the leading edge of the material. As a result, the Knudsen correction factor, b, obtained from the Felt 1 simulations is higher than that obtained from Borner *et al.*,[5] even though the material temperature in both the calculations is 300 K. According to the Klinkenberg theory, the b values from higher temperature simulations must scale with the lower temperature b^* calculations as $\frac{b}{b^*} = \frac{\mu\sqrt{T}}{\mu^*\sqrt{T^*}}$. Borner et al.[5] have shown that for simulations with different material temperatures, the scaling ratio of $\frac{b/b^*}{(\mu\sqrt{T})/(\mu^*\sqrt{T^*})}$ is close to unity, i.e., the ratio of b/b^* is equal to the ratio of $(\mu\sqrt{T})/(\mu^*\sqrt{T^*})$. Applying this scaling relationship,[5] we find that substituting the b value obtained from

CHAOS for the TT Morgan felt calculations and the average of the initial gas and surface temperature, i.e., T=(2000+300)/2=1150 K, the ratio of $\frac{b/b^*}{(\mu\sqrt{T})/(\mu^*\sqrt{T^*})} = 0.93$. Thus, the b obtained from CHAOS satisfies the temperature and viscosity scaling ratio within the 10% uncertainty error involved in the material characterization studies.

Table 3: Permeability comparison of Morgan felt in IP and TT

Solver	**CHAOS** Felt 2 (IP)	**CHAOS** Felt 1 (TT)	**Borner** *et al.*[5] (TT)
Sample size (μm^3)	1032×1032×1032	1032×1032×1032	520×520×520
Surface Temperature (K)	300	300	310
Initial gas temperature (K)	2000	2000	310
$K_o \times 10^{-12}$m^2	271.8	209.9	195
Knudsen correction factor, b (Pa)	5,896.69	7,027.15	1,403

B. Effect of orientation and sample size on permeability of FiberForm

The variation of the permeability force, F, with average pressure for the 1 mm^3 Form 1 case is shown in Fig. 3(a). The TT continuum permeability obtained by taking the slope of the F vs P_{av} line for Form 1 case is 31.96×10^{-12}m^2 and the Knudsen correction factor, b=23,357.3 Pa. Comparing our results with those from Panerai *et al.*,[9] it is found that the continuum permeability predicted from the CHAOS DSMC simulations with 1 mm^3 is 38% smaller compared to the K_o from the experiments that used a 22 mm^3 sample. This difference in the $K_{o,TT}$ values from DSMC and experiments may be due to the large microstructure variablity of FiberForm and due to the possible difference in the microstructure of our computational sample and the large specimen used in the experiments. Experimental data[9] have also shown that the uncertainty in the material permeability are up to ± 10% and that long-range variabilities in the fibrous structure within the material may affect the TT material properties.

Figure 3(b) shows the variation of F with average pressure for the 1 mm^3 FiberForm in

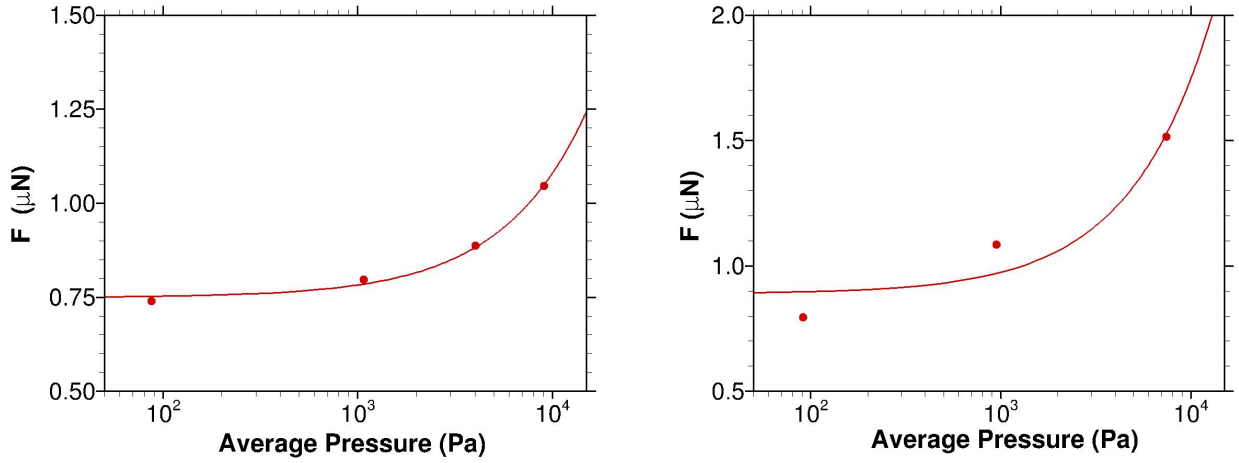

(a) F versus average pressure in the TT direction. $K_{o,TT}$=31.96×10^{-12} m^2, b=23,357.3 Pa.

(b) F versus average pressure in the IP direction. $K_{o,IP}$=85.84×10^{-12} m^2, b=10,350.69 Pa.

Figure 3: Continuum permeability, K_o and Knudsen correction factor, b, of cases Form 1 and Form 2 in TT and IP.

the IP direction, i.e., for Form 2 test case. The slope of this line resulted in an IP K_o of 85.84×10^{-12} m^2 and b=10,350.69 Pa. Due to the anisotropic fiber orientation, the material permeability in the IP direction is nearly 2.5 times higher than the TT K_o. Similar to the Morgan felt calculations, the less permeable TT direction results in more gas-surface interactions, higher slip correction and therefore higher b values compared to the more permeable IP orientation. The K_o and b values from Form 2 case are compared in Table 4 with the values obtained from the experiments[9] as well as the DSMC computations performed by

Table 4: Permeability comparison of FiberForm in the In-Plane (+x) direction

Solver	**CHAOS Form 2 case**	**Experiments**	**Borner *et al.*[5]**
Sample size (mm)	1.032×1.032×1.032	21×21×21	0.52×0.52×0.52
Initial T_g and T_s	T_g=2000 K, T_s=300 K	T_g=300 K, T_s=300 K	T_g=310 K, T_s=310 K
K_o×10^{-12}m^2 in TT	85.84	112	97.54
Knudsen correction factor, b (Pa) in TT	10,350.69	1,408	1,517.5

Borner *et al.*[5] on a $(520\mu\text{m})^3$ material sample. It was found that the IP K_o from CHAOS for the 1 mm^3 sample is 24% smaller than the IP K_o obtained from the experiments,[9] and 12% smaller than the results obtained from the DSMC computations performed by Borner *et al.*[5] The Knudsen correction factor, b, from CHAOS simulations is higher than the b value obtained from the experiments as well as the DSMC computations performed with T_g=T_s=300 K. This is because, b depends on the gas temperature and for the Form 2 test case, the initial gas and surface temperatures were 2000 and 300 K, respectively, as shown earlier in Tab. 1.

Table 5: Permeability comparison of FiberForm in the through-thickness (-z) direction

Solver	**CHAOS Form 1 case**	**CHAOS Form 3 case**	**CHAOS Form 4 case**	**Borner *et al.*[5]**
Sample size (µm^3)	1032×1032×1032	1032×1032×1032	520×520×520	520×520×520
Initial T_g (K)	2000	1319	1319	1319
Surface temp. (K)	300	1319	1319	1319
$K_o\times10^{-12}$m^2	31.96	32.95	38.81	52.08
b (Pa)	23,357.3	45,402	40,118	12,198

To determine the effect of gas temperature on the continuum permeability, we performed simulations for the Form 3 case, with initial gas and surface temperature at 1319 K, similar to the DSMC calculations performed by Borner *et al.*[5] in the TT direction. The F versus average pressure values obtained for this thermal equilibrium Form 3 case are shown in Fig. 4. When the initial gas and surface temperature are equal, the continuum permeability in the TT direction was 32.95×10^{-12} m^2, which is similar to the K_o obtained for Form 1 case with different T_g and T_s shown in Fig. 3(a) and compared in Table 5. It is not surprising to see that the bulk continuum permeability of the material remains unchanged with initial gas or surface temperature, since it is strictly a microstructure dependent material property. But, as discussed earlier, the Knudsen correction factor, b, depends on the gas properties and we see that for the Form 3 case with T_g=T_s=1319 K, the b value is nearly twice that

of the Form 1 case with T_s at 300 K and initial T_g=2000 K. Using Form 3 reference values of $b^* = 45,402$ Pa and $T^* = 1319$ K, and Form 1 values of $b = 23,357$ K, and $T = (1/3) * 2000 + (2/3) * 300 = 866.6$ K, in the scaling ratio, we find that $\frac{b/b^*}{(\mu\sqrt{T})/(\mu^*\sqrt{T^*})} = 0.89$, which is 11% below unity, or close to the 10% uncertainty of material characterization studies. Note that, the temperature T used in the computation of the scaling ratio is a weighted average of the initial gas temperature of $T_g = 2000$ K and surface temperature of $T_s = 300$ K. The weights for the gas and surface temperature are 1/3 and 2/3 respectively, because the region of the computational domain consisting of the diffusely reflecting material surface is $2/3^{rd}$ of the computational domain, resulting in gas temperature equal to 300 K in that region. Since Morgan felt is more permeable that Fiberform, is allows the high temperature gases to penetrate through the material more easily. Therefore, a weighting factor of 1/2 was used to compute the average temperature used in the scaling relation for the Felt 1 calculations, discussed earlier in Sec. III A.

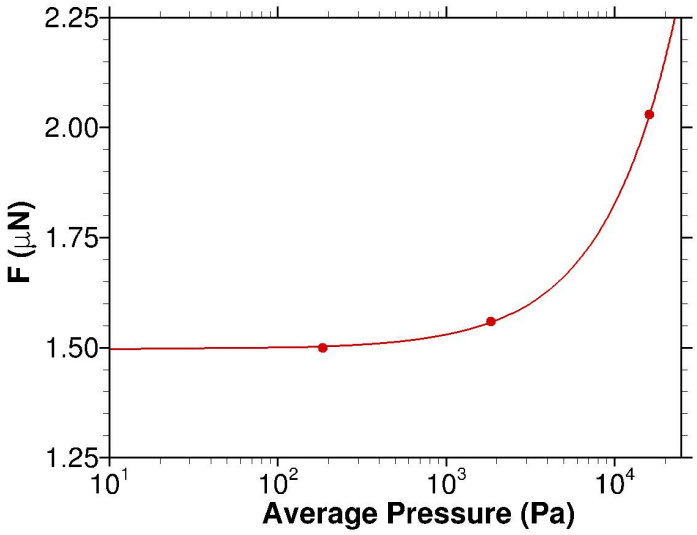

Figure 4: F versus average pressure for 1 mm^3 FiberForm in the TT direction for T_{gas}=T_{surf}=1319 K, i.e., Form 3 case. $K_{o,TT}$=32.95×10^{-12} m^2, b=45,402 Pa.

To understand the effect of sample size on the permeability calculations, we performed

DSMC simulations i.e., Form 4 case, with a smaller material sample of (520×520×520) μm^3 with initial gas and surface temperature at 1319 K. The variation of F values with average pressure for Form 4 case is compared with the experiments performed for 22 mm^3 sample with the same gas and surface temperature in Fig. 5. The continuum permeability obtained for the Form 4 case is K_o=38.81×10^{-12} m^2 which is nearly 25% less than the K_o obtained from the experiments in the TT direction. This difference in TT permeability obtained from the computations and experiments may be due to the large density variation of the material in the TT direction.[9] Further, the permeability force, F, obtained from the CHAOS DSMC calculations is higher than that obtained from the experiments for a given average pressure. For the same gas and surface temperature as well as material sample size of 520 μm^3, Borner *et al.*[5] obtained a value of 52.08×10^{-12} m^2 from their DSMC simulations, similar to the experiments which used an even larger material sample of 22 mm^3.

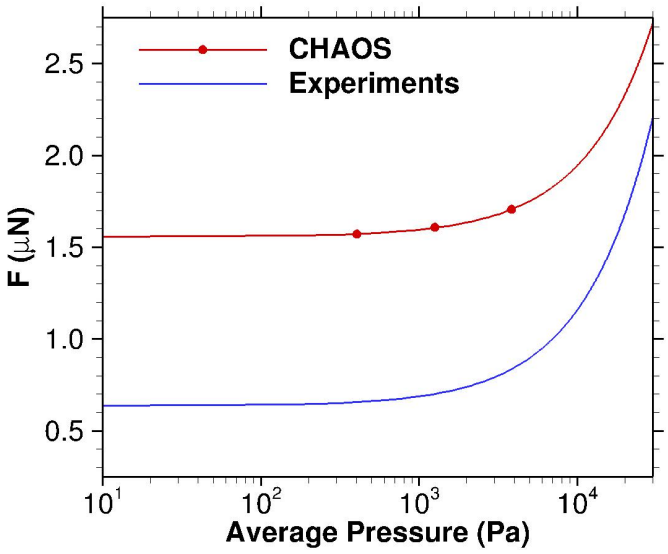

Figure 5: Variation of F with average pressure for 520 µm^3 FiberForm sample in the TT direction for T_{gas}=T_{surf}=1319 K, i.e., Form 4 case. $K_{o,TT}$=38.81×10^{-12} m^2, b=40,118 Pa.

C. Hydraulic tortuosity factor in a pressure driven flow

The hydraulic tortuosity, τ_h, is defined as the square of the ratio of the effective tortuous gas streamline through the material, l_t, to the shortest straight path, l, which is also equal to the depth of the material, in cases discussed here. This ratio is equivalent to the velocity ratio,[12–15]

$$(\tau_h)_i = \left(\frac{l_t}{l}\right)^2 = \left(\frac{< u >}{< u_i >}\right)^2 \tag{3}$$

where, $< u >$ is the average speed of the gas particles, and $< u_i >$ is the average value of the velocity component in the i^{th} direction, within the material. From the steady-steady results obtained from the CHAOS DSMC simulations, u and u_i are sampled in each leaf node, where $u = (u_x^2 + u_y^2 + u_z^2)^{(1/2)}$. By taking the average of $< u >$ and $< u_i >$ over all the cells within the material, the bulk hydraulic tortuosity factor for the i^{th} direction is computed by substituting the sampled values of $< u >$ and $< u_i >$ in Eq. 3. The variation of τ_h with average pressure within the 1 mm^3 FiberForm and Morgan felt materials in the TT and IP orientation are compared in Fig. 6. For both, Morgan felt and FiberForm, the TT orientation is more tortuous compared to the IP orientation. It can be observed that the effective path of the gas is more tortuous through the rigid FiberForm microstructure compared to the Morgan felt microstructure. This is consistent with the smaller permeability obtained in the TT direction compared to the IP direction. In addition, the hydraulic tortuosity factor is found to increase with increasing average pressure. As the flow becomes more continuum-like, the twistiness of the effective streamline path is larger due to smaller velocity slip at the material surface, compared to the lower pressure cases. At lower pressure the higher slip effects reduce the curvature of the effective streamline and the effective tortuosity. It was also found from Fig. 6 that the hydraulic tortuosity factor, τ_h remained constant above 4,000 Pa. When the pressure increases, the gas-gas collisions dominate compared to the gas-surface

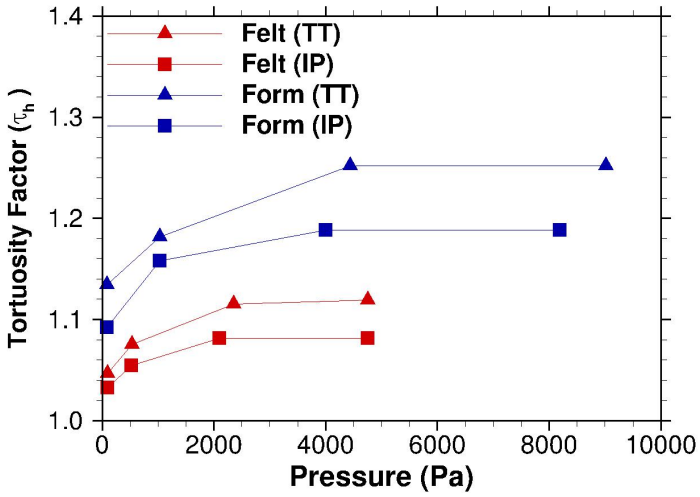

Figure 6: Variation of hydraulic tortuosity factor, τ_h with average pressure within the material.

collisions, the effective flow path does not change, maintaining the τ_h at a constant value beyond 4,000 Pa. The length of the streamlines, l_t, was also computed using the commercial software, Tecplot, and the ratio of $(l_t/l)^2$ resulted in tortuosity factors within 2% of that obtained from the square of the velocity ratio. Since the hydraulic tortuosity factor, τ_h,

Table 6: Comparison of hydraulic and diffusive tortuosity factors

Tortuosity	**CHAOS** τ_h=$(< u > / < u_i >)^2$	**Panerai** *et al.*[4] τ_d
FiberForm (TT)	1.25	1.225
FiberForm (IP)	1.18	1.15
Morgan felt (TT)	1.12	1.08
Morgan felt (IP)	1.08	1.053

from the simulations did not vary beyond 4,000 Pa, the τ_h, for the highest pressure case is compared with the continuum diffusion tortuosity factor, τ_d obtained by Panerai at al.[4] in Tab. 6. It can be seen that the maximum difference between the τ_h computed using the velocity ratio method and the diffusive tortuosity factor, τ_d is within 3%.

Table 7: Tortuosity comparison for FiberForm in the through-thickness direction, using velocity ratio and particle tracking

Pressure (Pa)	**Velocity Ratio,** τ_h=$(< u > / < u_i >)^2$	**Particle Tracking,** l_d/l
1012	1.18	2.22
9018	1.25	3.4

In addition, 100,000 gas particles were tracked from the time they enter the FiberForm material in the TT direction, to the time they leave the material, to determine the average length of their kinetic trajectories throughout the material. The ratio of average length of the particles trajectories, l_d, to the length of the material, l, for FiberForm at 1,012 and 9,018 Pa average pressures are compared with the TT hydraulic tortuosity factor, τ_h, in Tab. 7. It was found that, on average, the gas particle trajectory is 2.2 and 3.4 times longer than the material length, for 1,012 and 9,018 Pa pressures, respectively. The length of the particle trajectory is found to increase with increase in the pressure, similar to the trend observed for the τ_h, but, the ratio of kinetic trajectory length to material size is larger than τ_h. The particle trajectories includes both gas-gas and gas-surface collisions, and all the displacements it undergoes when trapped within the material, whereas the hydraulic tortuosity factor, τ_h, only accounts for the effective length of the streamline as the gas flows through the porous region due to pressure gradient.

IV. Conclusion

The permeability of hydraulic tortuosity factor of two types of carbon preforms, namely, Morgan Felt and FiberForm, are computed using a multi-GPU hybrid MPIC-CUDA Direct Simulation Monte Carlo (DSMC) solver. It was found that for both the anisotropic materials, the in-plane orientation is more permeable than the through-thickness orientation. Compared to Morgan Felt, FiberForm is less permeable, in both, through thickness and

in-plane directions. On the contrary, the Knudsen correction factor is higher for Fiberform compared to the Felt, because, the gas undergoes higher gas-surface interactions in the less permeable Fiberform, resulting in higher slip, and therefore higher correction factors. The hydraulic tortuosity was higher for the FiberForm sample compared to Morgan Felt sample, and it was also found that the through-thickness orientation is more tortuous compared to the in-plane orientation.

Acknowledgments

We are grateful for the funding support provided by NASA through the Grant NNX 16AD12G. This research is part of the Blue Waters sustained-petascale computing project, which is supported by the National Science Foundation (awards OCI-0725070 and ACI-1238993) and the state of Illinois. Blue Waters is a joint effort of the University of Illinois at Urbana-Champaign and its National Center for Supercomputing Applications.

References

[1]Agrawal, P., Chavez-Garcia, J. F., and Pham, J., "Fracture in phenolic impregnated carbon ablator," *Journal of Spacecraft and Rockets*, Vol. 50, No. 4, 2013, pp. 735–741.

[2]Lachaud, J., Cozmuta, I., and Mansour, N. N., "Multiscale approach to ablation modeling of phenolic impregnated carbon ablators," *Journal of Spacecraft and Rockets*, Vol. 47, No. 6, 2010, pp. 910–921.

[3]Panerai, F., Ferguson, J., Lachaud, J., Martin, A., Gasch, M. J., and Mansour, N. N., "Analysis of fibrous felts for flexible ablators using synchrotron hard x-ray micro-tomography," *8th European Symposium on Aerothermodynamics for Space Vehicles*, 2015.

[4]Panerai, F., Ferguson, J. C., Lachaud, J., Martin, A., Gasch, M. J., and Mansour, N. N., "Micro-tomography based analysis of thermal conductivity, diffusivity and oxidation behavior of rigid and flexible fibrous insulators," *International Journal of Heat and Mass Transfer*, Vol. 108, 2017, pp. 801–811.

[5]Borner, A., Panerai, F., and Mansour, N. N., "High temperature permeability of fibrous materials using direct simulation Monte Carlo," *International Journal of Heat and Mass Transfer*, Vol. 106, 2017,

pp. 1318–1326.

[6]Bird, G., *Molecular gas dynamics and the direct simulation of gas flows*, Oxford Engineering Science Series, Clarendon Press, 1994.

[7]Jambunathan, R. and Levin, D. A., "Advanced parallelization strategies using hybrid MPI-CUDA octree DSMC method for modeling flow through porous media," *Computers & Fluids*, Vol. 149, 2017, pp. 70–87.

[8]Top500.org, "Top 500, List," `https://www.top500.org/lists/2016/06/`, 2016, [Online; accessed 20-August-2016].

[9]Panerai, F., White, J. D., Cochell, T. J., Schroeder, O. M., Mansour, N. N., Wright, M. J., and Martin, A., "Experimental measurements of the permeability of fibrous carbon at high-temperature," *International Journal of Heat and Mass Transfer*, Vol. 101, 2016, pp. 267–273.

[10]Scheidegger, A. E., *Physics of flow through porous media*, No. 532.5 S2 1974, University of Toronto, 1963.

[11]Marschall, J. and Milos, F. S., "Gas permeability of rigid fibrous refractory insulations," *Journal of Thermophysics and Heat Transfer*, Vol. 12, No. 4, 1998, pp. 528–535.

[12]Epstein, N., "On tortuosity and the tortuosity factor in flow and diffusion through porous media," *Chemical Engineering Science*, Vol. 44, No. 3, 1989, pp. 777–779.

[13]Kawagoe, Y., Oshima, T., Tomarikawa, K., Tokumasu, T., Koido, T., and Yonemura, S., "A study on pressure-driven gas transport in porous media: from nanoscale to microscale," *Microfluidics and Nanofluidics*, Vol. 20, No. 12, 2016, pp. 162.

[14]Civan, F., "Effective Correlation of Apparent Gas Permeability in Tight Porous Media," *Transport in Porous Media*, Vol. 82, No. 2, Mar 2010, pp. 375–384.

[15]Shin, C., "Tortuosity correction of Kozeny's hydraulic diameter of a porous medium," *Physics of Fluids*, Vol. 29, No. 2, 2017, pp. 023104.